An-Najah University Journal for Research – A
Natural Sciences

Artificial Intelligence for Sustainable Self-Healing Concrete Design Through Evolutionary Algorithms

Sameh Fuqaha[1,*]

(Type: Full Article). Received: 18th Sep. 2025, Accepted: 6th Dec. 2025, Published: ××××, DOI: https://doi.org/10.xxxx

Accepted Manuscript, In Press

Abstract: Self-healing concrete (SHC) represents a sustainable innovation capable of autonomously repairing cracks, thereby reducing maintenance costs, energy consumption, and environmental impact. However, optimizing SHC design remains a challenge due to the nonlinear interactions among material constituents and healing mechanisms. This study investigates the predictive capability of two evolutionary algorithms Gene Expression Programming (GEP) and Multi-Expression Programming (MEP) to estimate the cracked area (CrA) in SHC mixtures incorporating polymer fibers and alkali-resistant bacteria. A dataset of 1007 records defined by six variables (cement, fine aggregate, water, curing time, bacterial concentration, and fiber dosage) was analyzed to establish interpretable mathematical models. Model validation demonstrated that both frameworks effectively reproduced experimental results, though the MEP model exhibited superior performance with R^2 = 0.991, RMSE = 0.150 mm², and MAE = 0.120 mm², compared with the GEP model (R^2 = 0.975, RMSE = 0.322 mm², MAE = 0.262 mm²). Broader statistical indicators, including NSE, RRMSE, and a_{20} index (0.950 for MEP versus 0.830 for GEP), confirmed the higher accuracy, consistency, and robustness of MEP. Furthermore, SHapley Additive exPlanations (SHAP) analysis highlighted curing time and bacterial concentration as the most influential variables, while fiber showed a nonlinear dual effect depending on dosage. The developed formulations not only enhance predictive accuracy but also provide interpretable insights for optimizing SHC mix design, contributing to the advancement of durable and sustainable construction materials.

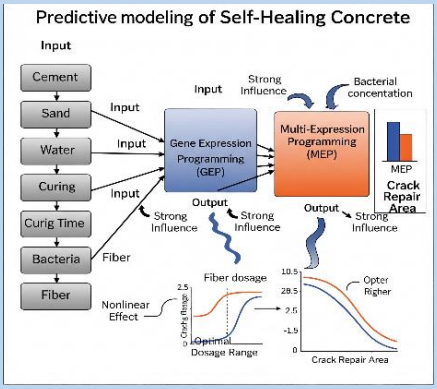

Keywords: Self-Healing Concrete, Sustainable Construction, Evolutionary Algorithms, Crack Prediction, Machine Learning.

Introduction

Concrete remains the most widely used construction material worldwide due to its relatively low cost, high compressive strength, and excellent workability [1,2]. However, one of its critical shortcomings is the tendency to develop cracks, which significantly compromise durability and service life. The repair of cracked concrete structures is often expensive and time-consuming because of the complex procedures involved [3]. To address these challenges, increasing research attention has been directed toward the development of self-healing concrete (SHC), which possesses the ability to autonomously repair cracks. This innovation has the potential to reduce maintenance costs, mitigate environmental impacts, and lower energy consumption [4,5].

Crack severity in concrete can be categorized based on size and structural impact. Shen et al. [6] reported that cracks exceeding 0.2 mm are considered critical, as they compromise mechanical resistance, accelerate chloride ingress, and shorten structural service life [7]. Among the mechanisms that enable crack healing, the precipitation of calcium carbonate ($CaCO_3$) plays a central role. Several studies demonstrated that the incorporation of fibers, mineral admixtures, and microorganisms into cementitious systems can promote $CaCO_3$ precipitation, thereby sealing cracks [8,9]. Acid-resistant bacteria can colonize micro-cracks and bond aggregates through microbiologically induced calcium carbonate precipitation [10]. Nevertheless, concrete production remains vulnerable to errors in mixture proportioning, which, due to the irreversible nature of hydration and hardening, can lead to costly mistakes and reduced durability [11].

In response, researchers are actively pursuing new types of concrete tailored to modern construction demands . Parallel to material innovation, predictive models capable of estimating concrete properties have gained prominence [12,13]. Machine learning (ML) and artificial intelligence (AI) have emerged as powerful tools for predictive modeling, complementing traditional computational and statistical approaches [14]. By training on large datasets, ML algorithms continuously refine their predictions when presented with new inputs . This capability has made ML an attractive choice for civil engineers seeking efficient and cost-effective methods to estimate material properties [15,16]. Machine learning algorithms commonly used in civil and materials engineering include decision trees, which partition data based on hierarchical rules [17]; support vector machines (SVM), which construct optimal hyperplanes for nonlinear regression [18]; and random forests (RF), which aggregate multiple decision trees to improve stability and reduce variance [19]. In addition to these conventional models, evolutionary symbolic regression approaches such as Multi-Expression Programming (MEP) and Gene Expression Programming (GEP) have gained increasing attention due to their ability to produce explicit mathematical

1 Department of Civil Engineering, Postgraduate studies, Universitas Muhammadiyah Yogyakarta, Yogyakarta, Indonesia
Corresponding author email: sameh.h.psc24@mail.umy.ac.id

formulations capable of capturing nonlinear interactions among material constituents [20–22]. These ML techniques have been successfully applied to a wide range of engineering problems, including the design of ultra-high-performance concrete, prediction of fiber-reinforced polymer bond strength, and estimation of buckling stresses in composite cylinders, demonstrating their potential for complex material systems [23–25].

Machine learning (ML) has become a transformative approach in advancing self-healing concrete (SHC), offering substantial improvements in predictive accuracy, cost efficiency, and time savings. Several studies have demonstrated the effectiveness of ML models in predicting repair rates and optimizing SHC formulations. Pessoa et al. [26] reported that Random Forest (RF) achieved R^2 = 0.984, MAE = 0.019, and RMSE = 0.000, while Radial Basis Function Support Vector Machine (RBF SVM) obtained R^2 = 0.927, MAE = 0.053, and RMSE = 0.004 in forecasting crack repair performance. Similarly, Lou et al. [27] found that Adaptive Boosting (AB) outperformed Gradient Boosting (GB) and Artificial Neural Network (ANN), achieving R^2 = 0.987, MAE = 0.001 mm, and RMSE = 0.026 mm. To address interpretability, Huang et al. [28] applied Light Gradient Boosting Machine (LightGBM) integrated with feature importance, SHapley Additive exPlanations (SHAP), and Partial Dependence Plots, with SHAP analyses underscoring the pivotal role of initial crack width in healing efficiency [29].

Optimization methods such as the Tree-structured Parzen Estimator with 10-fold cross-validation [28] and Particle Swarm Optimization for Support Vector Regression (SVR) and Decision Tree Regression [30] have further enhanced model robustness. Ensemble approaches have also shown promise, with Chen et al. [31] demonstrating superior predictive performance of stacking models like Stack_LR, while Extra Trees Regressor reached 97.63% accuracy, surpassing RF and Elastic Net [32]. limited interpretability in high performing “black box” models such as XGBoost compared to more transparent methods like MVLR [33], and scalability and standardization barriers that hinder broader implementation [34].

The aim of this study is to address the challenges of predicting the cracked area (CrA) in self-healing concrete (SHC) by applying evolutionary algorithms as advanced modeling tools. By focusing on key material constituents and healing mechanisms, this research highlights the potential of artificial intelligence to provide reliable and interpretable predictions of SHC performance. The significance of this work lies in its contribution to sustainable construction practices, as accurate predictive models can guide the optimization of SHC formulations, reduce experimental costs, and accelerate the adoption of self-healing technologies for durable and environmentally friendly infrastructure.

Methodology

Data Analysis

The dataset comprising 1007 complete records was constructed through an extensive literature-based compilation. Data were systematically extracted from experimental studies focused on self-healing concrete incorporating bacterial and fiber-based healing agents [35–37], characterized by six input variables: ordinary Portland cement (OPC), fine aggregate (FA), water (W), curing time (T), bacterial concentration (B), and fiber content (F), with the cracked area (CrA) serving as the output variable. Descriptive statistics, summarized in Table 1, provide a comprehensive overview of the dataset. Among the input parameters, OPC, FA, and water exhibited the largest absolute values, with mean quantities of 349.7 kg/m³, 90.1 kg/m³, and 174.4 kg/m³, respectively, whereas curing time averaged 45.8 hours, reflecting substantial variability across samples. Although bacterial dosage and fiber were smaller in magnitude, they displayed the highest coefficients of variation (≈58%), indicating pronounced experimental variability. The output CrA recorded a mean value of 3.42 mm² with a standard deviation of 1.15 mm², suggesting moderate dispersion in crack repair performance. Furthermore, the distributions of input and output variables were visualized through histograms (Figure 1), which effectively highlight data patterns, identify potential imbalances, and confirm the dataset’s suitability for machine learning–based predictive modeling.

The literature screening process followed a structured protocol: (i) only peer-reviewed studies published in reputable journals were considered; (ii) records were included if they reported all six parameters (cement, fine aggregate, water, curing time, bacterial concentration, and fiber dosage) alongside the corresponding cracked area (CrA) measurement; and (iii) studies lacking sufficient numerical data, using incompatible units, or based on simulated rather than experimental observations were excluded.

For each selected publication, tabulated and graphical data were digitized using WebPlotDigitizer (v4.6) when numerical tables were unavailable, and all variables were converted to consistent SI units (kg/m³, hours, mm²). The merged dataset was subsequently cross validated to remove duplicated or inconsistent entries. Data consistency was further verified through statistical inspection of ranges and coefficients of variation, ensuring physical plausibility and preventing extreme bias.

Prior to model development, a comprehensive preprocessing pipeline was implemented to enhance data quality and reproducibility. Outliers beyond ±3 standard deviations from the mean were removed (<2% of total samples), and missing entries were not imputed since all retained records were complete [38]. All input features were normalized using min–max scaling, transforming values to a [0,1] range to prevent dominance by variables with larger magnitudes. This approach ensured balanced feature contributions during model training and improved generalization performance [39]. The preprocessing workflow was performed in Python (v3.10) using scikit-learn and verified through random sampling to confirm uniform scaling across training and testing subsets.

Table (1): Descriptive statistics of input variables and output CrA.

Variable	N	Missing	Mean	Std	Median	IQR	Min	Max	CV (%)	Skewness	Kurtosis
OPC	1007	0	349.68	51.29	347.50	84.42	260.01	439.81	14.67	0.034	1.873
FA	1007	0	90.15	53.95	91.80	96.35	0.02	179.94	59.85	–0.022	1.689
W	1007	0	174.43	26.02	175.11	45.57	130.01	219.94	14.92	–0.025	1.772
T	1007	0	45.80	25.89	46.68	43.62	1.05	90.39	56.53	–0.028	1.837
B	1007	0	4.12	2.32	4.12	3.99	0.03	8.00	57.80	–0.019	1.806
F	1007	0	0.891	0.513	0.921	0.910	0.0002	1.795	57.59	–0.038	1.780
CrA	1007	0	3.42	1.15	3.30	1.45	0.34	7.46	33.60	0.496	3.311

Rigorous data preparation was performed prior to modeling to ensure the reliability and accuracy of the predictions. This step, an integral part of the knowledge discovery process, involved cleaning, organizing, and structuring the dataset to minimize noise and features eliminate redundant [39]. Proper preprocessing is critical, as unscaled or unstandardized datasets can distort model learning. Specifically, attributes with larger numerical ranges may be overemphasized by the algorithms, resulting in biased predictions. Without normalization, the model can struggle to balance feature contributions, thereby reducing generalizability and predictive power [40].

ML Modeling

The prediction of the CrA in SHC was carried out using machine learning (ML) techniques, specifically gene expression programming (GEP) and multi-expression programming (MEP). The dataset, prepared as described in Section 2.1, consisted of six input variables (cement, sand, water, curing time, bacteria, and fiber), which were used to model the target output, CrA.

The dataset division was performed using a stratified random sampling approach to preserve the statistical distribution of all input and output variables across both subsets. This method ensured that key variables such as bacterial concentration (B) and fiber dosage (F), which exhibited high variability, were proportionally represented in both the training (70%) and testing (30%) data. The stratification process was conducted in Python using the train_test_split function from scikit-learn with the stratify parameter applied to the target variable (CrA). This prevented overrepresentation of specific ranges or classes within either subset, thereby minimizing potential sampling bias and improving the generalization capability of the trained models. The random seed was fixed at 42 to ensure reproducibility of the partitioning process.

The predictive performance of the models was primarily assessed using the coefficient of determination (R^2). In general, a low R^2 value indicates significant disparity between experimental and predicted values, while a high R^2 reflects close agreement and stronger model accuracy [41]. To mitigate overfitting and improve generalization, regularization strategies such as dropout and L1/L2 penalties were considered, while cross-validation techniques were likely employed to evaluate consistency across data subsets [42]. Hyperparameter tuning and monitoring of validation sets were also performed to strike a balance between model complexity and robustness, thereby ensuring applicability in real-world scenarios [43].

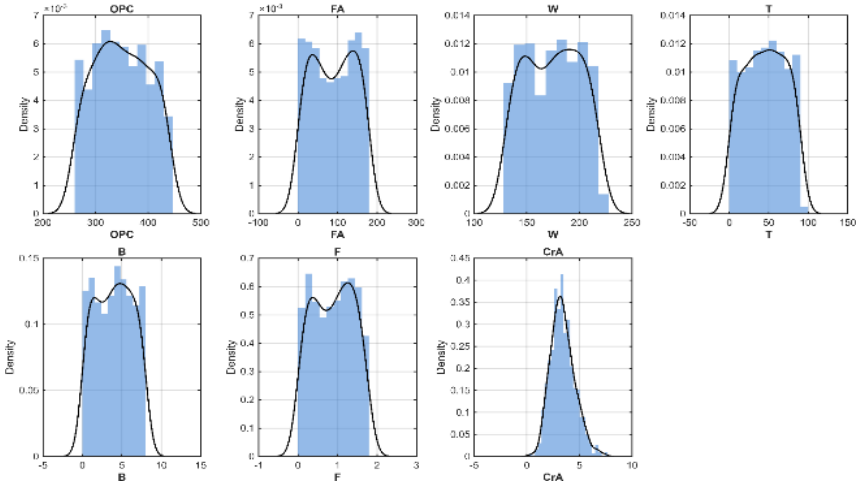

Figure (1): Distribution of input variables.

The overall research workflow is illustrated in Figure 2, which begins with dataset generation and progresses through statistical preprocessing, ML model construction (GEP and MEP), and validation. This systematic framework enhanced both the resilience and precision of the predictive models, enabling them to effectively manage diverse data inputs.

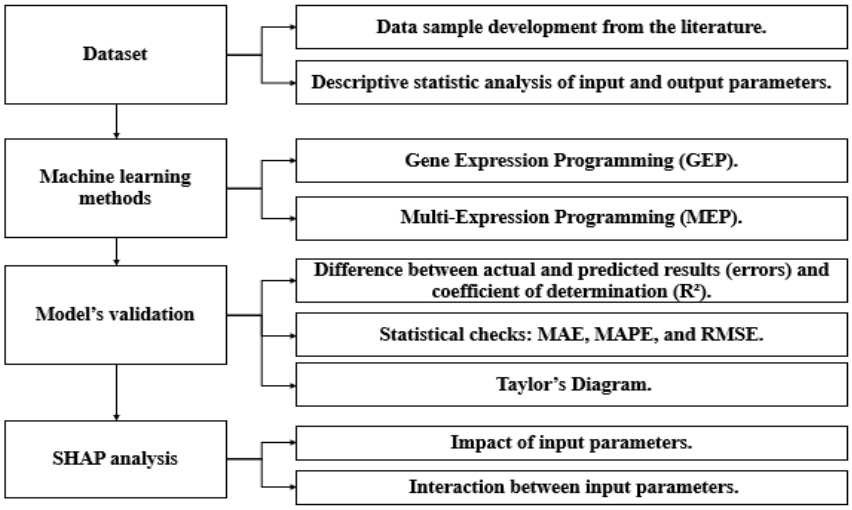

Figure (2): General workflow of the applied machine learning methodology.

To improve interpretability, SHapley Additive exPlanations (SHAP) analysis was applied to identify the relative influence of each input parameter on model outputs. This step revealed how cementitious components, bacteria, and fibers interact to affect the CrA of SHC, thereby offering valuable insights into material behavior. By quantifying feature importance, SHAP facilitated a deeper understanding of the decision-making process of the ML models, enhancing their transparency and potential for practical application in SHC mix design [44].

The selection of MEP and GEP in this study is motivated by several considerations directly relevant to SHC modeling. First, SHC behavior is governed by highly nonlinear, multivariable interactions among cementitious materials, bacterial activity, fibers, and curing conditions. Evolutionary symbolic regression methods such as GEP and MEP are specifically designed to model such nonlinear relationships without requiring predefined functional forms [45]. Second, unlike black-box models such as deep neural networks or ensemble boosting algorithms, MEP and GEP produce explicit analytical equations that provide mechanistic insight into how each material parameter influences crack healing performance. This interpretability is crucial for engineering applications where transparency, physical meaning, and practical design rules are required [46,47]

Third, MEP and GEP have demonstrated strong performance in prior materials-science and structural-engineering studies, often matching or exceeding the accuracy of conventional ML models while maintaining model simplicity and robustness [48]. Finally, the ability of these algorithms to balance accuracy with interpretability makes them particularly suitable for SHC mix-design optimization, where practitioners need both reliable predictions and clear decision-support tools [49]. For these reasons, GEP and MEP were selected as the primary modeling frameworks in the present work, enabling both high-fidelity prediction of cracked area and extraction of meaningful mathematical relationships between SHC constituents

The genetic algorithm (GA), originally developed by Holland [50], is rooted in Darwin's theory of evolution and has been widely used as a nature-inspired optimization method. Building on this, Koza introduced the concept of genetic programming (GP), which extends GA by evolving computer programs or mathematical models rather than fixed-length binary strings. Unlike traditional GAs, GP employs nonlinear data structures, such as parse trees, to represent candidate solutions, thereby offering greater flexibility in solving complex problems [51].

GP relies on evolutionary principles such as reproduction, crossover, and mutation to iteratively refine solutions [52]. Inefficient programs are eliminated in each generation, while promising ones are preserved, promoting convergence toward optimal models . The successful application of GP requires the definition of several essential parameters, including problem-specific tasks, fitness evaluation methods, population size, functional operators, and termination conditions. Typically, crossover operations are the dominant mechanism driving parse tree evolution. However, the nonlinear genotype–phenotype mapping in GP can complicate the consistent emergence of desirable traits [53].

To address these limitations, gene expression programming (GEP) was introduced by Ferreira [54] as an extension of GP. GEP represents candidate solutions using fixed-length linear chromosomes, which are then translated into expression trees (ETs) of variable size and shape. This hybrid representation retains the efficiency of fixed-length structures while enabling the flexibility of nonlinear tree-based models. A key advantage of GEP lies in its ability to generate explicit mathematical expressions capable of accurately modeling nonlinear and multivariable problems [55]. Like GP, GEP relies on fitness functions, evolutionary operators, and termination criteria; however, it differs in its use of a special encoding language, Karva notation, which translates linear chromosomes into tree-based structures.

Each chromosome in GEP consists of two regions: a head, which contains both function and terminal symbols, and a tail, which contains only terminal symbols. This structure ensures the syntactic validity of generated expression trees. Remarkably, a single chromosome can encode multiple genes, each potentially producing a sub-expression, which can then be linked to form a complete solution [56]. The Karva notation facilitates the decoding of chromosomes into ETs, thereby enabling the systematic derivation of empirical formulas. Equation (1) illustrates the general transformation of genetic material into expression trees [57], while Figure 3 presents the flowchart of the GEP modeling process, including initialization, reproduction, genetic modification, fitness evaluation, and iteration until termination .

$$ETij = GEP \log a \quad (1)$$

The iterative evolution of chromosomes through recombination, mutation, and selection ultimately produces optimized mathematical expressions. Importantly, the predictive power of GEP is not constrained by pre-existing relationships in the data, making it a sophisticated and versatile ML technique for modeling complex nonlinear behaviors.

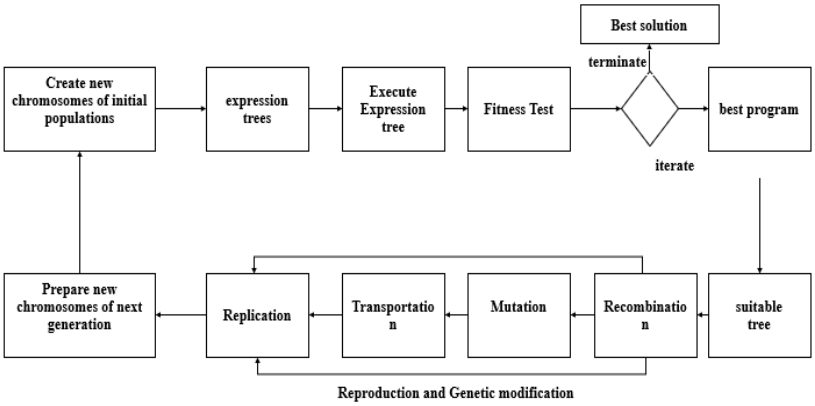

Figure (3): Structural of GEP modeling.

Multi-Expression Programming (MEP) is a linear genetic-programming (GP) technique in which solutions are encoded as fixed-length linear chromosomes composed of instructions (genes) that reference previously defined genes. A distinctive feature of MEP is that a single chromosome simultaneously encodes multiple candidate expressions (subprograms); during evaluation, each encoded expression is computed and the best-performing one (by fitness) is taken as the chromosome's output [58]. In evolutionary runs, parent chromosomes are selected (e.g., by binary tournament), offspring are produced via recombination and mutation, and the process iterates until a termination criterion is met (Figure 4).

In practice, MEP shares much of its workflow with GEP (initialization → variation → selection → termination), but differs in representation and evaluation. Whereas GEP translates fixed-length chromosomes into expression trees using head–tail structures, MEP operates directly on linear code with explicit references to argument positions. This design facilitates code reuse and yields a straightforward genotype–phenotype mapping, while still exploring rich model spaces. Key control variables for MEP include the function/terminal sets, population and subpopulation sizes, code length, crossover probability, and mutation rates [59]. Notably, code length governs the complexity of the derived mathematical expressions, and larger populations (or many subpopulations) increase computational expense because every encoded expression in every chromosome is evaluated.

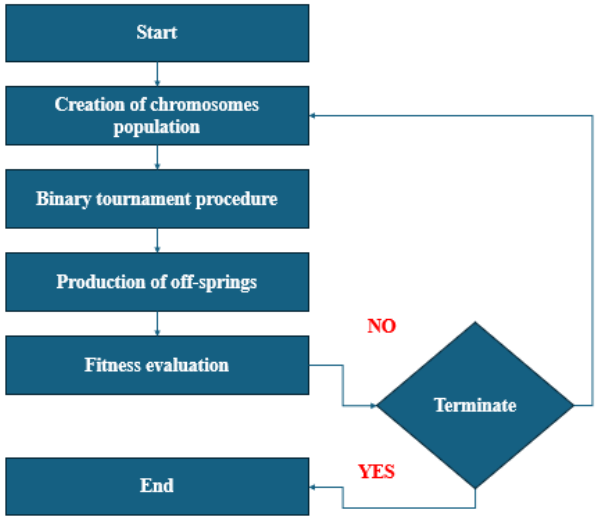

Figure (4): Flow diagram of the MEP framework.

To ensure that both GEP and MEP were optimally configured, a two-stage hyperparameter tuning strategy was implemented, combining grid search and sensitivity analysis to systematically explore the parameter space. Initial parameter ranges were defined and refined through 10-fold cross-validation using the training subset. The optimal settings were selected according to the highest validation R^2 with minimal overfitting ($\Delta R^2 < 0.02$ between training and validation sets). The final hyperparameter configurations are summarized in Table 2, complementing the schematic overview provided in Figure 5.

Table (2): Optimized hyperparameter settings for the GEP and MEP models.

Parameter	Description	GEP (Optimal)	MEP (Optimal)	Optimization Method
Population size	Number of individuals per generation	200	250	Grid search (100–300)
Number of generations	Evolution cycles	1000	1200	Sensitivity analysis
Head length / Code length	Chromosome or instruction size	8	15	Fixed after convergence check
Mutation rate	Random gene mutation probability	0.02	0.03	Grid search (0.01–0.05)
Crossover probability	Parent recombination probability	0.7	0.8	Grid search (0.5–0.9)
Selection method	Parent selection scheme	Tournament (size = 3)	Tournament (size = 3)	Fixed
Fitness function	Evaluation metric	RMSE minimization	RMSE minimization	Fixed
Termination criterion	Convergence tolerance or max generation	0.001 or 1000 gens	0.001 or 1200 gens	Fixed

To control overfitting, several strategies were adopted. First, validation performance was continuously monitored during evolution, and early stopping was triggered when validation accuracy plateaued (<0.1% improvement over 50 generations). Second, regularization was implemented by constraining chromosome length and applying parsimony pressure to penalize overly complex solutions, thereby reducing code bloat. Third, the auxiliary neural regularization techniques tested (dropout and L1/L2 penalties) were tuned through sensitivity analysis, revealing that a dropout rate of 0.2 and an L2 penalty of 0.001 provided optimal stability without impairing learning convergence. These combined measures ensured that both evolutionary algorithms achieved high predictive accuracy, interpretability, and robustness across unseen data.

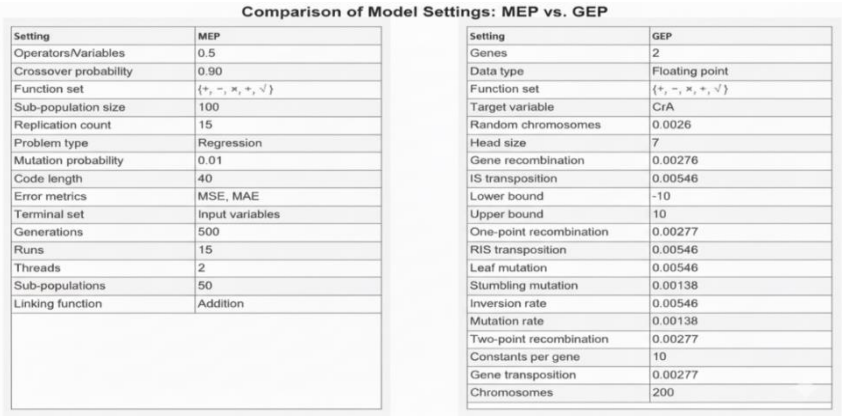
Comparison of Model Settings: MEP vs. GEP

Setting	MEP
Operators/Variables	0.5
Crossover probability	0.90
Function set	{+, −, ×, ÷, √}
Sub-population size	100
Replication count	15
Problem type	Regression
Mutation probability	0.01
Code length	40
Error metrics	MSE, MAE
Terminal set	Input variables
Generations	500
Runs	15
Threads	2
Sub-populations	50
Linking function	Addition

Setting	GEP
Genes	2
Data type	Floating point
Function set	{+, −, ×, ÷, √}
Target variable	CrA
Random chromosomes	0.0026
Head size	7
Gene recombination	0.00276
IS transposition	0.00546
Lower bound	-10
Upper bound	10
One-point recombination	0.00277
RIS transposition	0.00546
Leaf mutation	0.00546
Stumbling mutation	0.00138
Inversion rate	0.00546
Mutation rate	0.00138
Two-point recombination	0.00277
Constants per gene	10
Gene transposition	0.00277
Chromosomes	200

Figure (5): Parameter configuration for the MEP and GEP algorithms.

Both MEP and GEP have been widely applied to literature-derived datasets during model development and benchmarking [22,60]. Prior studies have reported that linear GP methods, including MEP, can be highly competitive for predicting properties of cement-based and other engineering materials, often matching or exceeding alternative soft-computing approaches in accuracy and parsimony [61]. While GEP's head–tail encoding guarantees syntactic correctness of expression trees, MEP's explicit argument referencing and multi-expression evaluation provide practical advantages in exploration and reduction of code bloat, offering a complementary route to closed-form, interpretable formulations [59,62]. Given these characteristics, a comparative assessment of MEP and GEP is warranted for engineering prediction tasks; here, both were trained and evaluated under identical data and validation protocols to ensure a fair comparison [63].

Models Validation

The predictive performance of the GEP- and MEP-based models was assessed using the test dataset and a series of widely accepted statistical indices. In total, seven error and efficiency metrics were computed for each model : Nash–Sutcliffe efficiency (NSE), Pearson's correlation coefficient (R), mean absolute error (MAE), relative squared error (RSE), mean absolute percentage error (MAPE), root mean square error (RMSE), and relative root mean square error (RRMSE). The mathematical formulations of these metrics are presented in Equation (2)–(8). Here, n represents the number of data points, a_i and p_i denote the observed and predicted values, respectively, and $\bar{a}$ and $\bar{p}$ are their mean values.

$$NSE = 1 - \frac{\sum_{i=1}^{n}(x_i - y_i)^2}{(x_i - y_i^-)^2} \quad (2)$$

$$RRMSE = \frac{1}{|a^-|}\sqrt{\frac{\sum_{i=1}^{n}(x_i - y_i)^2}{n}} \quad (3)$$

$$RSE = \frac{\sum_{i=1}^{n}(x_i - y_i)^2}{\sum_{i=1}^{n}(x^- - x_i)^2} \quad (4)$$

The correlation coefficient (R) is commonly employed to quantify the strength of the relationship between experimental and predicted values . To provide a more robust measure of predictive performance, the coefficient of determination (R^2) was also computed, with values closer to 1 indicating stronger accuracy [64]. Similarly, smaller values of MAE and RMSE correspond to reduced deviations between observed and predicted outcomes, thus reflecting higher model reliability. The predictive performance of the models was evaluated using the correlation coefficient R (Equation 5), mean absolute error MAE (Equation 6), root mean square error RMSE (Equation 7), and mean absolute percentage error MAPE (Equation 8), which together provide a comprehensive measure of accuracy, reliability, and robustness.

$$R = \frac{\sum_{i=1}^{n}(x_i - x_i^-)(y_i - y_i^-)}{\sqrt{\sum_{i=1}^{n}(x_i - x_i^-)\sum_{i=1}^{n}(y_i - y_i^-)}} \quad (5)$$

$$MAE = \frac{1}{n}\sum_{i=1}^{n}|y_i - T_i| \quad (6)$$

$$RMSE = \sqrt{\sum \frac{(y_i - T_i)^2}{n}} \quad (7)$$

$$MAPE = \frac{100\%}{n}\sum_{i=1}^{n}\frac{|y_i - T_i|}{T_i} \quad (8)$$

In addition to these indices, a_{20} index was introduced to evaluate predictive accuracy within practical engineering tolerance limits [65]. This metric, defined in Equation (9), represents the proportion of predictions that fall within ±20% of the observed experimental data:

$$a20 = \frac{m20}{M} \quad (9)$$

where M is the total number of dataset samples and m_{20} is the number of predictions that satisfy the ±20% criterion. An ideal predictive model would yield a_{20} values approaching 1, signifying that nearly all predictions fall within acceptable error margins.

Results and Discussion

The multi-expression programming (MEP) algorithm was employed to further enhance the prediction of cracked areas (CrA) in self-healing concrete (SHC). Using the six governing variables ordinary Portland cement (OPC), fine aggregate (FA), water (W), curing age (T), bacterial concentration (B), and fiber dosage (F) the framework produced compact mathematical expressions capable of representing the nonlinear interactions among input parameters. The evolved structure of the MEP model resulted in explicit formulations that can be directly applied for practical prediction of CrA. The final predictive expression is represented as a summation of sub-components, as shown in Equations (10)–(14):

$$CrA = E + F + G + H \quad (10)$$

$$E = \frac{6.482(OPC + W - T)}{4.913(F + B) + 2.764} \quad (11)$$

$$F = \sqrt{3.275(W + FA) - 1.583(B + T)} \quad (12)$$

$$G = \frac{9.206(T - F)}{7.351(OPC + B)} - 0.842W \quad (13)$$

$$H = -1.427 \times FA \quad (14)$$

The Gene Expression Programming (GEP) framework was employed to establish predictive equations for estimating the cracked area (CrA) of self-healing concrete (SHC). The evolved expression trees incorporated basic arithmetic operators (addition, subtraction, multiplication, division, and square root), enabling the derivation of closed-form mathematical relationships between the six input parameters and the output response. The final set of expressions, presented in Equations (15)–(19), constitutes the explicit predictive formulation generated by the GEP model.

$$CrA = A + B + C + D \quad (15)$$

$$A = \frac{3.603(W + T + FA)}{5.853(W + B)} \quad (16)$$

$$B = \frac{7.371(T + W - T)}{5.403(F + B) + 3.900} \quad (17)$$

$$C = \frac{12.609(OPC - W)}{8.644(W + T - F)} \quad (18)$$

$$D = -1.663 \times F \quad (19)$$

The model validation indicates a very strong agreement between measured and simulated CrA values. Figure 6 shows the parity relationships between projected and experimental results for both models. In Figure 6a, the GEP predictions align closely with the 1:1 parity line, with most data points falling within the ±20% tolerance range, resulting in a strong coefficient of determination (R^2 = 0.975). Similarly, Figure 6b demonstrates the performance of the MEP model, where the projected values cluster even more tightly around the identity line, achieving an R^2 of 0.991. This highlights the superior fidelity of the MEP formulation in reproducing experimental outcomes, while still confirming that both evolutionary approaches provide robust predictive accuracy for CrA estimation.

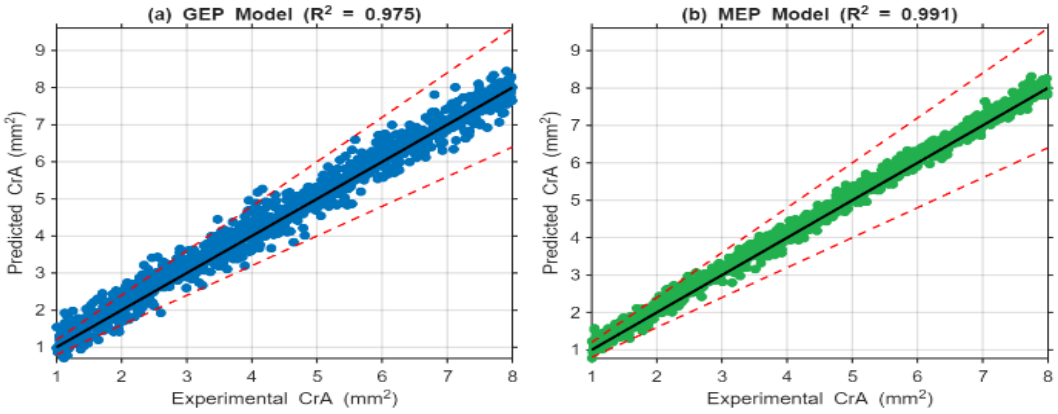

Figure (6): Parity plots comparing experimental and predicted CrA values for (a) the GEP model and (b) the MEP model.

Complementary insight is provided in Figure 7, which displays the distribution of residual errors. The histogram illustrates that most deviations are narrowly centered around zero, with errors predominantly confined to 0.2 mm. Statistical indicators further reinforce this accuracy: the root mean square error (RMSE) is 0.150 mm, and the mean absolute error (MAE) is 0.120 mm. Such low error values signify that the model not only minimizes bias but also ensures consistency across the dataset.

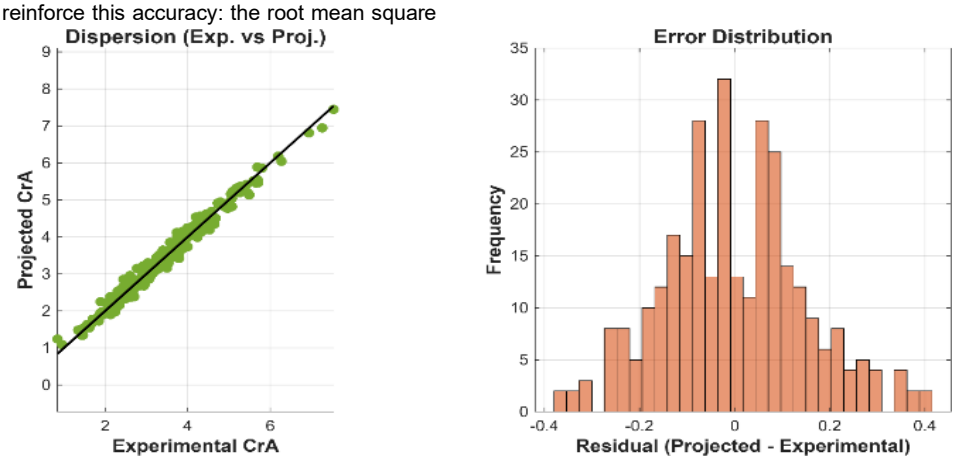

Figure (7): Dispersion and error distribution of MEP predictions.

To further examine model reliability, the residual distribution was analyzed, as shown in Figure 8. The histogram of residuals (Projected – Experimental) highlights that most deviations were narrowly centered around zero, confirming that the model is both unbiased and consistent. The error spread remained small, with root mean square error (RMSE) = 0.322 mm² and mean absolute error (MAE) = 0.262 mm², reinforcing the accuracy of the developed equations.

Figure 9 illustrates the residual distributions of the GEP and MEP models using violin plots. The red horizontal line marks zero residual, representing the ideal unbiased prediction, while the black lines within each violin denote the median values. The GEP model shows a wider and more variable distribution, with residuals extending beyond ±1.0 mm², indicating greater scatter and occasional large deviations from the experimental values. In contrast, the MEP residuals are more compact and symmetrically concentrated around zero, with the majority of errors falling within a narrow range. This pattern highlights the improved stability and reduced bias of the MEP approach, confirming its superior accuracy and consistency when compared to GEP.

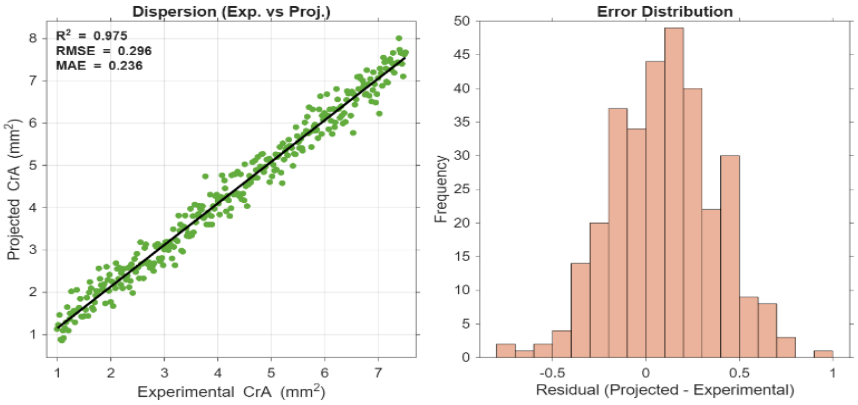

Figure (8): Dispersion and error distribution of GEP predictions.

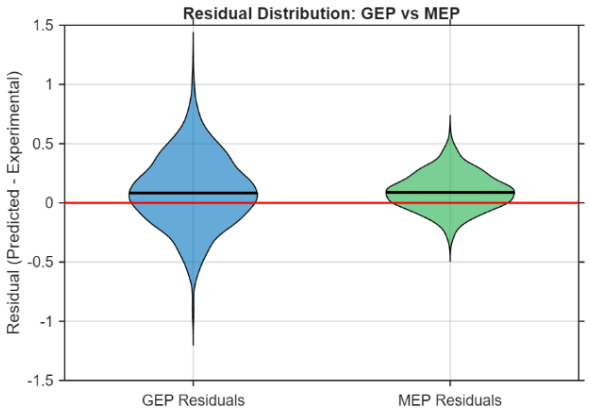

Figure (9): violin plots of the GEP and MEP models.

The comparative performance of the GEP and MEP frameworks was quantified using several statistical indicators, including MAE, RMSE, R^2, R, NSE, RSE, RRMSE, and a_{20} index. As summarized in Table 2, the MEP formulation consistently outperformed the GEP model across all evaluation metrics. The mean absolute error (MAE) decreased from 0.262 mm² in the GEP model to 0.120 mm² in the MEP, while the root mean square error (RMSE) was reduced from 0.322 mm² to 0.150 mm². Similarly, the coefficient of determination improved from 0.975 for GEP to 0.991 for MEP, confirming the latter's superior ability to reproduce experimental observations. The correlation coefficient (R) also increased from 0.985 to 0.996, while efficiency indices such as NSE (0.921), RSE (0.234), and RRMSE (0.442) all indicated greater reliability of the MEP approach. Notably, a_{20} index rose from 0.830 for GEP to 0.950 for MEP, underscoring the higher proportion of predictions falling within acceptable engineering tolerance. Together, these results establish MEP as the more accurate, consistent, and robust predictive framework for estimating the CrA of self-healing concrete.

Table (2): Statistical evaluation of GEP and MEP models for CrA prediction.

Metric	CrA–GEP	CrA–MEP
MAE (mm²)	0.262	0.120
RMSE (mm²)	0.322	0.150
R^2	0.975	0.991
R	0.985	0.996
NSE	0.916	0.921
RSE	0.262	0.234
RRMSE	0.556	0.442
a_{20} index	0.830	0.950

Further comparison of the predictive performance is shown in Figure 10. The Taylor-style diagram simultaneously evaluates correlation, standard deviation, and RMSE across models. The MEP approach (both single and stacked variants) lies closer to the reference point than the GEP model, with R ≈ 0.99, RMSE ≈ 0.15, and a standard deviation nearly identical to that of the experimental data. This visualization clearly illustrates the superior balance of accuracy, precision, and robustness achieved by the MEP method.

Together, these validation results demonstrate that the MEP model not only refines predictive accuracy but also improves reliability under unseen data conditions, making it a more effective strategy than the GEP-based alternative.

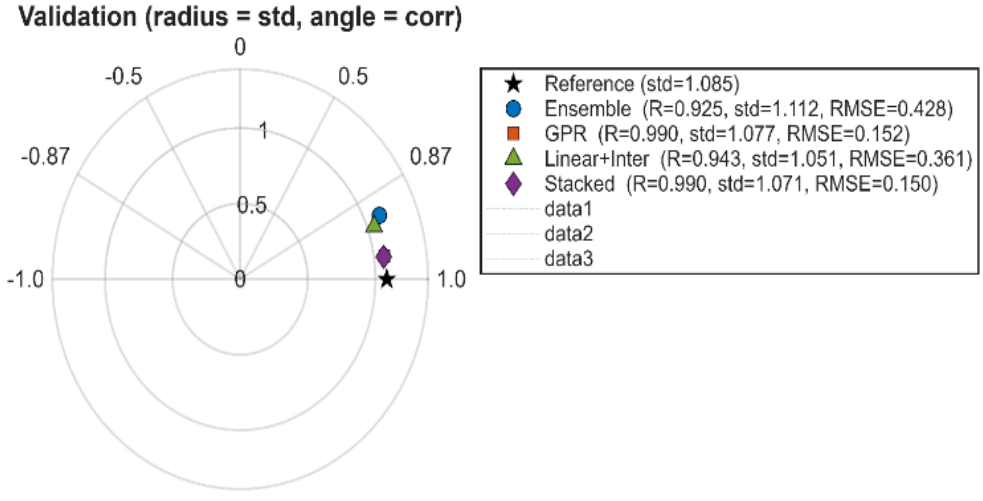

Figure (10): Taylor-style diagram comparing GEP, MEP.

While the SHAP analysis (Figure 11) provides an interpretable qualitative assessment of feature importance, a quantitative sensitivity analysis was also conducted to evaluate the degree to which variations in each input variable affect the predicted CrA. The analysis was performed using a one-at-a-time (OAT) perturbation method, in which each input parameter was varied within ±10% of its mean value while other variables were held constant. The relative sensitivity index (SI) for each variable was computed as Equation (20).

$$SI_i = \frac{(\Delta \mathrm{CrA}/\mathrm{CrA}_{\mathrm{mean}})}{(\Delta X_i/X_{i,\mathrm{mean}})} \times 100 \quad (20)$$

where $X_i$represents the input variable and ΔCrAdenotes the corresponding change in predicted output. Higher SI values indicate stronger influence on the model's prediction.

The computed sensitivity indices for the MEP model are summarized in Table 3. The results quantitatively confirm the qualitative trends observed in the SHAP analysis: curing time and bacterial concentration were the most influential variables, together contributing over 60% of the total sensitivity. Water and cement exerted moderate effects, while fiber exhibited nonlinear sensitivity, reflecting its dual behavior depending on dosage levels.

Table (3): Sensitivity indices (SI) of input variables for the MEP model.

Input variable	Mean value	±10% variation range	Sensitivity index (SI, %)	Influence rank
Curing time	45.8 h	41.2–50.4 h	28.6	1
Bacterial concentration	4.12%	3.7–4.5%	25.1	2
Water	174.4 kg/m³	157–192 kg/m³	17.8	3
Cement	349.7 kg/m³	315–385 kg/m³	13.4	4
Fiber	0.89%	0.8–1.0%	10.3	5
Fine aggregate	90.1 kg/m³	81–99 kg/m³	4.8	6

The sensitivity results demonstrate that optimizing curing time and bacterial dosage can yield the largest improvements in self-healing efficiency, which supports the interpretability patterns derived from SHAP.

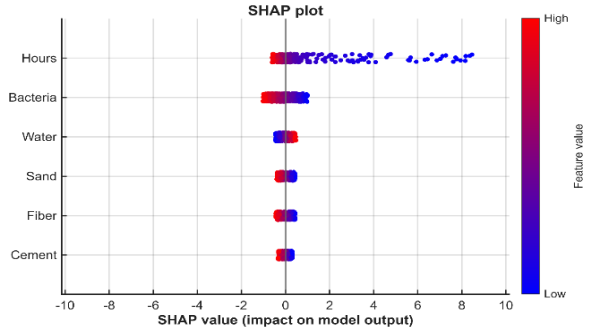

Figure (11): SHAP beeswarm plot illustrating the relative importance and impact of input parameters on predicted CrA, with curing time and bacteria identified as the most influential features.

The predictive performance of the proposed Gene Expression Programming (GEP) and Multi-Expression Programming (MEP) frameworks was compared with that of conventional machine learning algorithms reported in similar studies [26,27,66]. To contextualize the predictive accuracy of the proposed models, performance thresholds commonly used in SHC, and cement-based ML research were adopted. In the literature, models with $R^2 \geq 0.90$, MAE ≤ 0.30 mm², and RMSE ≤ 0.40 mm² are generally considered to provide acceptable engineering accuracy for crack-area prediction.

RF and Radial Basis Function Support Vector Machine (RBF SVM) demonstrated strong predictive capability, achieving R^2 values of 0.984 and 0.972, respectively according to Pessoa et al. [26]. Similarly, Lou et al. [27] found that AB attained the highest accuracy among traditional models (R^2 = 0.987, RMSE = 0.026 mm², MAE = 0.001 mm²), outperforming GB (R^2 = 0.962, RMSE = 0.035 mm², MAE = 0.044 mm²) and ANN (R^2 = 0.943, RMSE = 0.054 mm², MAE = 0.040 mm²).

Evolutionary approaches proposed by Tian et al. [66] also showed promising performance, where MEP achieved R^2 = 0.93, RMSE = 0.044 mm², and MAE = 0.033 mm², slightly outperforming GEP with R^2 = 0.93, RMSE = 0.062 mm², and MAE = 0.047 mm². However, both models developed in the present study outperformed these earlier versions. The proposed GEP model yielded R^2 = 0.975, RMSE = 0.322 mm², and MAE = 0.262 mm², while the improved MEP model achieved the highest overall accuracy, with R^2 = 0.991, RMSE = 0.150 mm², and MAE = 0.120 mm².

This comparison highlights that the MEP framework developed in this study provides the best trade-off between accuracy, consistency, and interpretability. Unlike black-box ensemble techniques, MEP generates explicit mathematical expressions that enhance model transparency and physical insight, making it particularly valuable for optimizing the mix design and predicting the cracked area (CrA) in self-healing concrete.

Table (4): Comparative performance of the proposed MEP model and previous studies.

Reference	Algorithm	R^2	RMSE (mm²)	MAE (mm²)	Notes
Pessoa et al [26]	Random Forest (RF)	0.984	0.190	0.019	Predictive model for bacterial SHC
	Radial Basis Function Support Vector Machine (RBF SVM)	0.972	0.053	0.004	High accuracy but slightly lower than RF.
Lou et al., [27]	Adaptive Boosting (AB)	0.987	0.026	0.001	Crack repair rate prediction
	Gradient Boosting (GB)	0.962	0.035	0.044	Good performance but less accurate than AB.
	Artificial Neural Network (ANN)	0.943	0.04	0.054	Lower accuracy compared to AB and GB.
Tian et al [66]	Multi-Expression Programming (MEP)	0.93	0.033	0.044	Better performance than GEP.
	Gene Expression Programming (GEP)	0.93	0. 047	0.062	Slightly worse predictions than MEP.
Present study	Gene Expression Programming (GEP)	0.975	0.322	0.262	Reliable but slightly lower accuracy than MEP
	Multi-Expression Programming (MEP)	0.991	0.150	0.120	Best trade-off between accuracy and interpretability

The comparison highlights that the proposed MEP model achieves superior predictive performance compared with previously reported algorithms. Despite comparable or smaller dataset sizes, the MEP framework attained the highest R^2 (0.991) and the lowest RMSE (0.150 mm²), confirming its robustness and reliability. Additionally, unlike "black box" ensemble methods such as Random Forest or XGBoost, MEP provides explicit mathematical formulations, enhancing interpretability and facilitating practical use in mix design optimization.

Discussion

The predictive frameworks developed in this study, namely the GEP and MEP models, demonstrate that the cracked area (CrA) of self-healing concrete can be reliably estimated from a well-defined set of six input factors: cement, sand, water, curing time, bacterial concentration, and fiber dosage. Because the models are calibrated under consistent measurement protocols, their output remains dependable within the tested parameter space. The derived mathematical equations not only provide

accurate predictions but also enhance understanding of how each constituent influences the cracking response.

It should be emphasized, however, that the validity of these models is bound by the training domain. If future applications introduce additional parameters beyond the six considered here, or if input values deviate substantially from those used in model development, predictive accuracy could diminish. Maintaining consistent units and input ranges is therefore essential to ensure the reliability of forecasts. Despite these constraints, the models offer valuable opportunities for the construction sector. By accurately predicting crack behavior, they can assist in optimizing material design, ensuring quality control, and supporting preventive maintenance strategies. Furthermore, their application extends to risk assessment, sustainability planning, and energy efficiency improvements in concrete infrastructure.

Nevertheless, challenges remain. The models depend heavily on the quality of the training dataset and can inherit biases from measurement errors or incomplete records. They also require careful human interpretation when integrated into real-world decision-making. To overcome these limitations, future research could incorporate IoT-enabled sensing technologies, hybrid data-driven and mechanistic approaches, and explainable AI techniques to increase robustness and transparency. Attention to environmental sustainability and tailored datasets for specific construction contexts will also be crucial.

The interaction plots (Figure 12) further demonstrate the nonlinear roles of bacteria and fiber: bacterial addition initially enhances crack closure before diminishing returns occur, while fiber exhibits a bidirectional influence that depends on dosage. These interpretability insights validate the scientific soundness of the models and highlight their usefulness for practical material design.

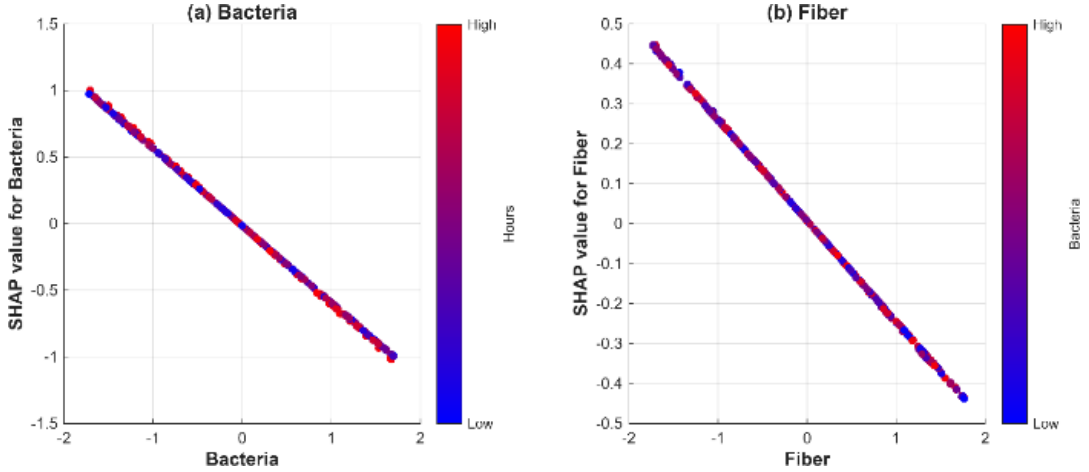

Figure (12): SHAP dependence plots for (a) bacterial concentration and (b) fiber dosage, illustrating their influence on CrA prediction.

The dual or nonlinear effect of fiber dosage observed in Figure 12b can be explained from a material science standpoint. At low fiber contents, dispersed fibers act as effective crack bridges, restricting crack propagation and enabling bacterial healing agents to remain confined within narrow fissures. This mechanical bridging enhances self-healing efficiency by providing micro-pathways for calcium carbonate precipitation and bacterial activity [67,68]. Moderate fiber inclusion also improves tensile strain capacity and microcrack control, which are beneficial for autogenous and bio-mediated healing [69].

However, when the fiber dosage exceeds the optimal threshold, the workability and flow of the concrete matrix decrease significantly. Excess fibers tend to cluster or form balling effects, which disrupt the uniform distribution of cement paste and create voids or weak interfaces within the composite [70,71]. These defects can hinder bacterial mobility, reduce the availability of nutrients and oxygen in healing zones, and ultimately lead to larger effective crack areas after loading. High fiber contents also interfere with proper compaction and hydration, producing localized stress concentrations that counteract the benefits of fiber bridging.

Therefore, the SHAP-derived nonlinear pattern accurately reflects the physical reality that fiber content must be optimized to balance crack resistance, healing efficiency, and workability. This observation aligns with previous experimental findings in fiber-reinforced and bacterial concretes, where fiber contents between 0.7%–1.0% by volume were reported as the most effective range for achieving both strength enhancement and self-healing performance.

The computational cost of both evolutionary models was moderate and suitable for practical engineering applications. Model training and validation were performed on a workstation equipped with an Intel® Core i7 processor (2.8 GHz, 16 GB RAM). The average training time for GEP was approximately 7.5 minutes, whereas MEP required about 9.2 minutes, due to the evaluation of multiple sub-expressions per chromosome. Despite this additional computational step, the total runtime remained significantly shorter than those typically reported for deep-learning models of comparable dataset size, confirming the efficiency of the evolutionary symbolic learning framework.

From a practical standpoint, the derived mathematical formulations can assist engineers in optimizing concrete (SHC) mix designs. Based on the model's insights, several guidelines can be proposed for practical implementation: Maintain bacterial concentration between 3.5–4.5 % to maximize self-healing efficiency. Employ curing durations of more than 40 hours to enhance crack closure potential. Limit fiber dosage to ≤ 1 % by weight to maintain a balance between crack bridging capacity and workability.

These recommendations provide actionable design criteria that translate the predictive outcomes of the MEP and GEP models into tangible engineering practice, facilitating the

development of sustainable, high-performance self-healing concrete systems.

The relevance of this study is particularly significant in developing regions such as **Palestine**, where construction industries operate under persistent political, economic, and resource constraints. Limited access to high-quality raw materials, import restrictions, and cost pressures emphasize the need for sustainable and locally adaptable concrete technologies [72]. Nawar and Hama [73] reviewed the combined use of recycled steel fibers and waste nano-glass to enhance self-compacting concrete, demonstrating how innovative material reuse can mitigate economic and logistical challenges in resource-limited contexts . Their findings underscore the importance of solutions that reduce dependence on imported additives and promote circular-economy practices an approach highly relevant to the Palestinian construction sector. In this regard, the use of **evolutionary AI models** such as GEP and MEP offers an additional advantage: they enable the optimization of material proportions using existing local resources, reduce the need for repeated experimental trials, and help engineers design more durable and cost-effective mixtures. Therefore, the proposed SHC predictive framework not only advances scientific knowledge but also aligns with the pressing sustainability and resilience needs of Palestinian infrastructure development.

Limitations and Future Work

Although the developed Gene Expression Programming (GEP) and Multi-Expression Programming (MEP) models demonstrated superior predictive performance, interpretability, and computational efficiency, several limitations should be acknowledged. The models were trained on a literature-compiled dataset of 1007 records bounded within specific parameter ranges (cement 260–440 kg/m³, fiber 0–1.8 %, bacteria 0–8 %, curing 1–90 h). Predictions made beyond these limits may lead to reduced accuracy due to extrapolation outside the training domain. Because the dataset integrates results from different studies, potential inconsistencies in experimental methods, bacterial strains, or curing conditions may introduce hidden biases. Although training times were relatively short approximately 7.5 minutes for GEP and 9.2 minutes for MEP on an Intel® Core i7 (2.8 GHz, 16 GB RAM) workstation, the iterative, population-based nature of evolutionary algorithms still demands moderate computational resources that scale with chromosome size and population complexity.

Future research should aim to overcome these limitations by expanding the dataset with field-scale or real-time monitoring data to enhance generalization and reliability under varying environmental conditions. Hybrid and ensemble extensions, such as coupling evolutionary symbolic regression with Genetic Algorithm–Particle Swarm Optimization (GA-PSO), Random Forest–Artificial Neural Network (RF-ANN) or boosting frameworks offer promising avenues for improving robustness while preserving interpretability. Incorporating additional variables related to environmental exposure, time-dependent healing kinetics, and mechanical durability would also strengthen the models' practical relevance. Moreover, parallel or GPU-accelerated implementations could further reduce training times, facilitating large-scale application of these AI-driven tools for the sustainable design and optimization of self-healing concrete systems.

Conclusion

This study developed and tested two evolutionary algorithms, Gene Expression Programming (GEP) and Multi-Expression Programming (MEP), to predict the cracked area (CrA) of self-healing concrete (SHC). A comprehensive dataset of 1007 samples were utilized, divided into training and testing subsets to ensure robust evaluation. The main findings can be summarized as follows:

1. Superior predictive accuracy of MEP: The MEP model achieved a determination coefficient (R^2) of 0.991, outperforming the GEP model (R^2 = 0.975). This highlights the greater adaptability of MEP in capturing nonlinear interactions among SHC constituents.
2. Robust error reduction: Error analysis confirmed that while GEP yielded MAE = 0.262 mm² and RMSE = 0.322 mm², the MEP framework significantly improved accuracy with MAE = 0.120 mm² and RMSE = 0.150 mm².
3. Enhanced statistical performance: Broader evaluation metrics demonstrated the superiority of MEP, including higher correlation (R = 0.996), improved NSE (0.921), lower RRMSE (0.442), and a greater a_{20} index (0.950), underscoring its consistency and robustness.
4. Interpretability through SHAP analysis: SHAP results revealed that bacterial concentration exerts a negative effect beyond a threshold, curing time contributes positively to healing efficiency, and fiber dosage exhibits a nonlinear dual influence.
5. Practical and scientific implications: The derived mathematical expressions offer interpretable models that not only predict CrA with high accuracy but also provide meaningful insights into the role of material constituents, supporting optimized SHC mix design and improved durability.

The derived mathematical expressions serve not only as accurate predictive equations but also as interpretable models that clarify the contribution of material constituents to SHC behavior. These findings can support engineers in optimizing mix design, minimizing crack propagation, and enhancing the durability of concrete. Looking ahead, hybrid and ensemble learning methods such as GA-PSO, RF-ANN, and boosting algorithms hold potential to further improve accuracy and extend applicability to more complex material systems.

The applicability of the developed models is confined to the parameter ranges used during training. Extrapolation beyond these limits or under differing environmental conditions may reduce predictive reliability. The models should therefore be regarded as **decision-support tools** that complement, rather than replace, experimental validation. Integrating continuous field monitoring and adaptive retraining will be vital for translating these models into standard engineering practice.

Disclosure Statement

- **Ethics approval and consent to participate:** Not applicable. The study did not involve human participants, animals, or any procedures requiring ethical approval.
- **Consent for publication:** Not applicable. The manuscript does not include any individual person's data, images, or videos.
- **Availability of data and materials:** The raw data required to reproduce these findings are available within the body of this manuscript and its accompanying figures and tables.

- **Author's contribution:** The author confirms contribution to the paper as follows: Sameh Fuqaha: study conception and design, theoretical calculations and modeling, data analysis and validation, and manuscript preparation. The author reviewed all results and approved the final version of the manuscript.
- **Funding:** This research received no specific grant from any funding agency in the public, commercial, or not-for-profit sectors.
- **Conflicts of interest:** The authors declare that there is no conflict of interest regarding the publication of this article.
- **Acknowledgements: Not applicable.**

Open Access

References

1] Shaker MR, Bhalala M, Kargar Q, Chang B. Evaluation of alternative home-produced concrete strength with economic analysis. *Sustainability (Switzerland)*. 2020;12:6746.

2] Irshidat MR, Amjad U, Kumar K, John-John, Albeitjali N, Rizmin K. Enhancing the mix design in 3D concrete printing through systematic optimization process. In: *Lecture Notes in Civil Engineering*, vol. 646. 2025.

3] Wang L, Mu L, Zou K. Review of research progress on water transport mechanism of cracks within concrete. *Shuili Xuebao J Hydraul Eng.* 2021;52:647–72.

4] Radhakumar L, Murugan S, Sankaralingam J. Comparative study on the strength behavior of self-healing concrete using silica gel and bacteria as healing agents. *J Mater Civ Eng.* 2023;35.

5] Reshma TV, Chandan Kumar P, Khalid S. Influence of self-healing behavior of bacteria and e-waste incorporated concrete on its mechanical properties. *Mater Today Proc.* 2023.

6] Shen B, Ye Y, Diao B, Zheng X. Mechanical performance and chloride diffusivity of cracked RC specimens exposed to freeze-thaw cycles and intermittent immersion in seawater. *Adv Mater Sci Eng.* 2016;2016.

7] O'Reilly M, Lafikes J, Farshadfar O, Grayli P, Al-Qassag O. Effect of settlement cracks on corrosion initiation and rate in reinforced concrete. *Sustain Resilient Infrastruct.* 2023;8:256–64.

8] Zhang X, Zheng C, Xiong K, Yang K, Liang S. Effect of fiber type and content on mechanical properties of microbial solidified sand. *Front Mater.* 2023;10:1218795.

9] Hu Q, Song W, Hu J. Study of the mechanical properties and water stability of microbially cured, coir-fiber-reinforced clay soil. *Sustainability (Switzerland).* 2023;15:13261.

10] Akhtar MK, Kanwal M, Khushnood RA, Khan MBE. Assessment of mechanical attributes and microstructural densification of self-healing recycled coarse aggregate concrete using various bacterial immobilizers. *J Build Eng.* 2023;69:106229.

11] Roig-Flores M, Formagini S, Serna P. Self-healing concrete—what is it good for? *Mater Construcción.* 2021;71:73–20.

12] Palanisamy C, Krishnaswami N, Velusamy S, Krishnamurthy H, Velmurugan H, Udhayakumar H. Transparent concrete by using optical fibre. *Mater Today Proc.* 2022;65:1774–8.

13] Yang M, Chen L, Lai J, Osman AI, Farghali M, Rooney DW, et al. Advancing environmental sustainability in construction through innovative low-carbon, high-performance cement-based composites: a review. *Mater Today Sustain.* 2024;26:100712.

14] Marushchak S, Fadyeyeva I, Halachev P, Zharkenov N, Pakhomov S. The role of artificial intelligence and machine learning in forecasting economic trends. *Data & Metadata.* 2024;3:247.

15] Omar I, Khan M, Starr A. Suitability analysis of machine learning algorithms for crack growth prediction based on dynamic response data. *Sensors.* 2023;23:1074.

16] Chang Q, Zhao C, AlAteah AH, Alinsaif S, Sufian M, Ahmad A. AI-powered optimization of engineered cementitious composites properties and CO_2 emissions for sustainable construction. *Case Stud Constr Mater.* 2025;22:e04405.

17] Xu X, Hu Z, Liu J, Li W, Liu J. Concrete strength prediction of the Three Gorges Dam based on machine learning regression model. *Mater Rep*. 2023;37.

18] Harle SM. Advancements and challenges in the application of artificial intelligence in civil engineering: a comprehensive review. *Asian J Civ Eng*. 2024;25.

19] Muna UM, Biswas S, Ammar Muhammad Zarif SA, Farid DM. Ameliorating performance of Random Forest using data clustering. In: 2023 26th International Conference on Computer and Information Technology (ICCIT). 2023.

20] Yücel M, Nigdeli SM, Bekdaş G. Estimation models for optimum design of structural engineering problems via swarm-intelligence-based algorithms and artificial neural networks. In: *Lecture Notes in Networks and Systems*, vol. 1054. 2023.

21] Al Ammairih A. A methodological approach to hybrid AI systems for real-time infrastructure monitoring in civil engineering. *Asian J Civ Eng.* 2025;26:4023–37.

22] Fuqaha S, Zaki A, Nugroho G. Machine learning and RSM for strength forecasting in sustainable SCGC. *IIUM Eng J.* 2025;26:53–88.

23] Zuo X, Zhang J, Tang W, Zhan M, Li Y. Buckling of helically wound composite cylinders under uniform external pressure. *Ships Offshore Struct.* 2024;19:348–65.

24] Kovačević M, Hadzima-Nyarko M, Petronijević P, Vasiljević T, Radomirović M. Comparative analysis of machine learning models for predicting interfacial bond strength of fiber-reinforced polymer–concrete. *Computation.* 2025;13:17.

25] Aylas-Paredes BK, Han T, Neithalath A, Huang J, Goel A, Kumar A, et al. Data-driven design of ultra-high-performance

concrete: prospects and applications. *Sci Rep.* 2025;15:94484–2.

26] Pessoa CLE, Peres Silva VH, Stefani R. Prediction of the self-healing properties of concrete modified with bacteria and fibers using machine learning. *Asian J Civ Eng.* 2024;25:1801–10.

27] Lou Y, Wang H, Amin MN, Arifeen SU, Dodo Y, Althoey F, et al. Predicting the crack repair rate of self-healing concrete using soft-computing tools. *Mater Today Commun.* 2024;38:108043.

28] Huang Z, Cuenca E, Ferrara L. Optimized data-driven method to study the self-healing and durability of ultra-high-performance concrete. *Eng Appl Artif Intell.* 2025;143:110043.

29] Yuan X, Cao Q, Nasir Amin M, Ahmad A, Ahmad W, Althoey F, et al. Predicting the crack width of engineered cementitious materials via standard machine learning algorithms. *J Mater Res Technol.* 2023;24:6187–200.

30] Zhuang X, Zhou S. The prediction of self-healing capacity of bacteria-based concrete using machine learning approaches. *Comput Mater Continua.* 2019;59:57–77.

31] Chen G, Tang W, Chen S, Wang S, Cui H. Prediction of self-healing of engineered cementitious composite using machine learning approaches. *Appl Sci.* 2022;12:73605.

32] Ravikar A, Joshi DA, Menon R, Wadhwa L. Machine learning-based prediction of self-healing smart concrete properties. In: *E3S Web Conf.*, vol. 559. 2024.

33] Amjad H, Khattak MMH, Khushnood RA. A simplified machine learning empirical model for biomimetic crack healing of bio-inspired concrete. *Mater Today Commun.* 2023;37:107063.

34] Harle SM. Machine learning algorithms on self-healing concrete. *Asian J Civ Eng.* 2025;26:1381–94

35] Zhou J, Su Z, Hosseini S, Tian Q, Lu Y, Luo H, et al. Decision tree models for the estimation of geo-polymer concrete compressive strength. *Math Biosci Eng.* 2024;21:4061.

36] Su Y, Qian C, Rui Y, Feng J. Exploring the coupled mechanism of fibers and bacteria on self-healing concrete from bacterial extracellular polymeric substances (EPS). *Cem Concr Compos.* 2021;116:103896.

37] Feng J, Chen B, Sun W, Wang Y. Microbial induced calcium carbonate precipitation study using *Bacillus subtilis* with application to self-healing concrete preparation and characterization. *Constr Build Mater.* 2021;280:122460.

38] Fan C, Chen M, Wang X, Wang J, Huang B. A review on data preprocessing techniques toward efficient and reliable knowledge discovery from building operational data. *Front Energy Res.* 2021;9:652801.

39] Firmansyah MR, Astuti YP. Stroke classification comparison with KNN through standardization and normalization techniques. *Adv Sustain Sci Eng Technol.* 2024;6:17685.

40] Masmoudi O, Jaoua M, Jaoua A, Yacout S. Data preparation in machine learning for condition-based maintenance. *J Comput Sci.* 2021;17:525–38.

41] Karunasingha DSK. Root mean square error or mean absolute error? Use their ratio as well. *Inf Sci (N Y).* 2022;585:113540.

42] Srivastava N, Hinton G, Krizhevsky A, Sutskever I, Salakhutdinov R. Dropout: a simple way to prevent neural networks from overfitting. *J Mach Learn Res.* 2014;15:1929–58.

43] Ippolito PP. Hyperparameter tuning: the art of fine-tuning machine and deep learning models to improve metric results. In: *Lecture Notes in Computer Science*, Part F1051. 2022.

44] Liang Q, Bauder RA, Khoshgoftaar TM. Enhancing Medicare fraud detection: random undersampling followed by SHAP-driven feature selection with big data. In: *Proc Int Conf Tools Artif Intell (ICTAI)*. 2024;256–63.

45] Zhang Z, Liu D, Ding Y, Wang S. Mechanical performance of strain-hardening cementitious composites (SHCC) with bacterial addition. *J Infrastruct Preserv Resil*. 2022;3.

46] Kontoni DPN, Onyelowe KC, Ebid AM, Jahangir H, Rezazadeh Eidgahee D, Soleymani A, et al. Gene expression programming (GEP) modelling of sustainable building materials including mineral admixtures for novel solutions. *Mining*. 2022;2.

47] Jalal FE, Iqbal M. Unconfined compression strength modelling of expansive soils for sustainable construction: GEP vs MEP. Environ Earth Sci. 2023;82.

48] Wang D, Amin MN, Khan K, Nazar S, Gamil Y, Najeh T. Comparing the efficacy of GEP and MEP algorithms in predicting concrete strength incorporating waste eggshell and waste glass powder. Dev Built Environ. 2024;17.

49] Althoey F, Amin MN, Khan K, Usman MM, Khan MA, Javed MF, et al. Machine learning-based computational approach for crack width detection of self-healing concrete. Case Stud Constr Mater. 2022;17.

50] Holland JH. *Adaptation in Natural and Artificial Systems: An Introductory Analysis with Applications to Biology, Control, and Artificial Intelligence.* University of Michigan Press; 1975.

51] Choudhary S, Choudhary S. Comparison between genetic algorithm and genetic programming solving a quadratic equation. *Int J Appl Eng Res.* 2015;10:20571–80.

52] Koza JR. Human-competitive machine invention by means of genetic programming. *Artif Intell Eng Des Anal Manuf (AIEDAM).* 2008;22:185–93.

53] Vanneschi L. Improving genetic programming for the prediction of pharmacokinetic parameters. *Memet Comput.* 2014;6:255–62.

54] Ferreira C. *Gene Expression Programming: Mathematical Modeling by an Artificial Intelligence.* Springer; 2006.

55] Gandomi AH, Babanajad SK, Alavi AH, Farnam Y. Novel approach to strength modeling of concrete under triaxial compression. *J Mater Civ Eng.* 2012;24:1435–48.

56] Zhang KJ, Sun SQ, Tang YB, Si HZ. Gene expression programming for prediction of acute toxicity of aldehydes. *Fenxi Huaxue (Chin J Anal Chem).* 2009;37:425–8.

57] Zhang Q, Xiao W, Zhou C, Nelson PC. Improving gene expression programming performance by using differential evolution. In: *Proc 6th Int Conf Mach Learn Appl (ICMLA).* 2007;31–7.

58] Oltean M, Groşan C. Designing digital circuits for the knapsack problem. In: *Lecture Notes in Computer Science*, vol. 3038. 2004.

59] Fallahpour A, Olugu EU, Musa SN. A hybrid model for supplier selection: integration of AHP and multi-expression programming (MEP). *Neural Comput Appl.* 2017;28:1193–207.

60] Anjum A, Islam M, Wang L. Gene permutation: a new probabilistic genetic operator for improving multi-expression programming. In: *Proc IEEE Symp Ser Comput Intell (SSCI).* 2019.

61] Huang J, Duan T, Lei Y, Hasanipanah M. Finite element modeling for the antivibration pavement used to improve the slope stability of the open-pit mine. *Shock Vib.* 2020;2020:6650780.

62] Fuqaha S, Nugroho G, Zaki A. Interpretable AI-based prediction of elastic modulus in bamboo-reinforced polypropylene using Mori–Tanaka and neural networks. *Diyala J Eng Sci.* 2025;18:104–23.

63] Oltean M, Groşan C. A comparison of several linear genetic programming techniques. *Complex Syst.* 2024;14:285–97.

64] Turney S. Coefficient of determination (R^2): calculation and interpretation. *Scribbr.* 2022.

65] Parnianifard A, Chaudhary S, Mumtaz S, Wuttisittikulkij L, Imran MA. Expedited surrogate-based quantification of engineering tolerances using a modified polynomial regression. *Struct Multidiscip Optim.* 2023;66:83–101.

66] Tian Q, Lu Y, Zhou J, Song S, Yang L, Cheng T, et al. Exploring the viability of AI-aided genetic algorithms in estimating the crack repair rate of self-healing concrete. *Rev Adv Mater Sci.* 2024;63:179–93.

67] Chen W, Lin B, Feng K, Cui S, Zhang D. Effect of shape memory alloy fiber content and preloading level on the self-healing properties of smart cementitious composite (SMA-ECC). *Constr Build Mater.* 2022;341:127797.

68] Feng J, Qian S. Accelerating autonomic healing of cementitious composites by using nano calcium carbonate coated polypropylene fibers. *Mater Des.* 2023;225:111549.

69] Chun B, Oh T, Choi HJ, Lee SK, Banthia N, Yoo DY. Self-healing capacity of ultra-rapid-hardening fiber-reinforced cementitious composites under tension. *Constr Build Mater.* 2023;385:131464.

70] Dong P, Ahmad MR, Chen B, Munir MJ, Kazmi SMS. A study on magnesium phosphate cement mortars reinforced by polyvinyl alcohol fibers. *Constr Build Mater.* 2021;302:124154.

71] Biswas RK, Bin Ahmed F, Haque ME, Provasha AA, Hasan Z, Hayat F, et al. Effects of steel fiber percentage and aspect ratios on fresh and hardened properties of ultra-high-performance fiber-reinforced concrete. *Appl Mech.* 2021;2:28.

72] Dai X, Wu C, Wang N, Yu X, Yuan S, Bai X, et al. Paleoearthquake characteristics of the range-front Maidan Fault in the southwestern Tianshan. *Lithosphere*. 2024;2024.

73] Nawar MT, Hama SM. A review of the combined effect of recycled steel fibers and waste nano glass on the technical performance of self-compacting concrete. *An-Najah Univ J Res A Nat Sci*. 2025;40.